

**Dependence of convective heat flux calculations on roughness lengths**

by John Schieldge

California Institute of Technology, Jet Propulsion Laboratory,

Terrestrial Science Element, Pasadena, CA 91109 USA

**Abstract.** The zero plane displacement height ( $d$ ) and aerodynamic roughness length ( $z_0$ ) can be determined separately for momentum, heat, and humidity by using a procedure based on the Levenberg-Marquardt method for solving non-linear equations. This procedure is used to analyze profile data previously collected by Lo (1977) in a forested area in Canada and by Morgan *et al* (1971) on a field at the University of California at Davis (UCD) in the United States. The UCD data base is used to show the effects of allowing for different roughness lengths ( $z_{0m}, z_{0h}, z_{0q}$ ) in calculating sensible and latent heat flux densities from bulk transfer coefficients.

## 1. Introduction

Accurate estimations of convective heat flux densities at the ground provide an important database for studies of atmospheric circulation at micro -, meso -, and synoptic scales as well as pertinent information for monitoring the soil heat and water balance of eco - and agro - systems. Many of the algorithms that are used to compute convective heat flux densities require a value for the aerodynamic roughness length of the surface. The aerodynamic roughness length characterizes the intensity of the momentum transfer from the atmosphere to the ground. Similar roughness lengths are defined to characterize the transfer of heat and water vapor between the ground and the air. The roughness lengths for momentum, heat, and moisture are usually assumed to be equal. (The displacement heights are also usually assumed to be equal or are neglected altogether). This assumption of equality facilitates the calculation of convective fluxes from the Monin-Obukhov equations for turbulent transport in the layers of air nearest the ground (i.e., the atmospheric surface layer). The penalty one pays for this assumption of equality is an additional uncertainty (over and above measurement errors and the assumption of horizontal homogeneity) in the estimation of the convective heat flux densities. In this paper, we test the proposition that convective heat flux densities can be computed by assuming equivalence of roughness lengths and displacement heights for momentum, heat, and moisture transfer in the atmospheric surface layer,

where  $\rho$  is the density of air,  $c_p$  is the specific heat capacity at constant pressure, and  $L_s$  is the latent heat of evaporation.

A number of methods have been developed to calculate convective fluxes and Monin-Obukhov parameters from profile measurements. Haenel (1993) generalized a non-linear iteration scheme of Robinson (1962) and applied the method to a data set of Lo's (1977) which consisted of profile measurements of winds and temperature over a forest. Haenel found that his method predicted the observed wind and temperature profiles as well, or better, than did the methods of Lo (1977) and Kramm (1989). Despite the success of Haenel's method in fitting surface layer profile data, it is based on the assumption that the roughness lengths for heat and momentum are equal, i.e.  $z_{0m} = z_{0h}$ . A number of studies have shown that there is a significant disparity between the values of  $z_{0m}$  and  $z_{0h}$  for many kinds of surfaces (cf. Brutsaert, 1982 for a summary). Therefore, any technique that is used to compute Monin-Obukhov parameters from profile measurements ought to account for any differences that might be realized among  $z_{0m}$ ,  $z_{0h}$ ,  $z_{0q}$ .

In this paper, we use another technique -to fit profile data to the Monin-Obukhov equations - that enables the determination of separate values of  $Z$ . for momentum, heat, and moisture transfer. This technique is an iterative procedure based on the Levenberg-Marquardt method of solving non-linear equations. In the following

sections, first, we present the method of analysis and demonstrate its effectiveness on an artificial set of wind and temperature profile data where the ratio  $z_{0m}/z_{0h}$  is allowed to vary ( $= 1, 10, 100$ ). Second, we apply the technique to profile data collected by various investigators from two sites in the United States and Canada. Finally, we analyze how convective heat flux densities (computed using bulk transfer coefficients) depend upon the values of  $z_{0m}$ ,  $z_{0h}$ ,  $z_{0q}$  assumed for a particular site.

## 2. Methodology

The Levenberg-Marquardt method is used to minimize non-linear regression functions that involve many parameters (Beale, 1967). In the case of the Monin-Obukhov equations, the regression functions are:

$$U_i = U(z_i; \mathbf{a}_u), \quad (6)$$

$$T_i = T(z_i; \mathbf{a}_t), \quad (7)$$

$$Q_i = Q(z_i; \mathbf{a}_q). \quad (8)$$

Each representation of  $U, T, Q$  depends upon  $z_i$  and a vector consisting of four or five parameters (e.g.,  $U$  depends upon  $\mathbf{a}_u$ :  $[z_{0m}, L, U^*, d_m]$ ). The Levenberg-Marquardt method is used to obtain that set of parameters that produce the best fit to the observed data. The approach is to minimize an objective function  $\gamma$

which is the sum of the squares of the residual between each fit ( $s_{fi}$ ) and the observed quantity ( $s_{oi}$ ) of U, T, or Q:

$$\gamma = \sum h_i^2, h_i = s_{fi} - s_{oi}. \quad (9)$$

Essentially, the approach is to minimize  $\gamma$  for each solution space, namely  $\mathbf{a} = \mathbf{a}_U, \mathbf{a}_T, \mathbf{a}_Q$ . This is done by the use of the method of steepest descent when the fit results in solutions far from the minimum, and a standard Newton-Raphson minimization procedure when the fit results in solutions close to the minimum. By differentiating  $\gamma$  twice, we obtain a gradient vector ( $\mathbf{f}$ ) of first derivatives of  $a_k$  ( $a_k$  represents a single element  $k$  of  $\mathbf{a}$ , e.g.  $Z_{0h}$ ), and a square symmetric matrix of second derivatives called the Hessian matrix ( $\mathbf{A}$ ). This enables us to compute the next step  $a_{k,j+1}$  in the minimization process:

$$a_{k,j+1} = a_{k,j} + [\lambda \mathbf{A}^{-1} \mathbf{A}^t \mathbf{f}]_k \quad (10)$$

Where  $a_{k,j}$  is the solution at the previous iteration,  $\lambda$  is a LaG range multiplier,  $\mathbf{A}^t$  is the transpose of  $\mathbf{A}$ ,  $\mathbf{I}$  is the  $m \times m$  identity matrix, and  $m$  is the number of parameters to be fitted (either four or five). The details of the Levenberg-Marquardt method are elaborated in a number of sources (e.g. Kuester and Mize, 1973; Press et al, 1986). Both references contain subroutines that can be used as the bases for a procedure to solve (1) through (3), but what must be supplied by the investigator is a set of derivatives of the functions to be fitted. This is described below.

GA  
double-former

To use the Levenberg-Marquardt method to fit observations of U,T,Q , we must differentiate the regression equations (7-8) with respect to each parameter ( $a_k$ ). This involves differentiating the diabatic correction factors (1) through (3) which have been represented in a number of ways. Hogstrom (1988) presented a comprehensive analysis of a number of representations of the  $\Psi_m$  and  $\Psi_h$  functions based on studies by various authors. We used the results of this analysis in our study, and also included the more recent representations of Brutsaert (1992). We found that the diabatic correction factors of Dyer (1 974) gave the best results in our fits of the data to (1) through (3). Below, we list the derivatives of U,T,Q with respect to  $\mathbf{a}$  for Dyer's (1 974) formulae, for unstable and stable conditions:

For unstable conditions, Dyer's (1 974) diabatic correction formulae are:

$$\phi_m = (1.0 - 16.0\zeta_i)^{-0.25} , \zeta_i < 0$$

$$\phi_h = \phi_m^2$$

$$\phi_q = \phi_h$$

$$\Psi_m(\zeta_i) = 2 \ln(1/\phi_m + 1) + \ln(1/\phi_m^2 + 1) - 2\tan^{-1}(1/\phi_m)$$

$$\Psi_h(\zeta_i) = 2 \ln(1/\phi_h + 1)$$

$$\Psi_q(\zeta_i) = \Psi_h(\zeta_i)$$

and for stable conditions:

$$\phi_q = \phi_h = \phi_q = 1 + 5\zeta_i,$$

$$\Psi_m(\zeta_i) = \Psi_h(\zeta_i) = \Psi_q(\zeta_i) = -5(\zeta_i - \zeta_{0i}),$$

where  $\zeta_{0i}$  is different for each mode of transfer (m,h,q).

The derivatives of equations 1 through 3 are:

Winds:

$$\partial U_i / \partial a_{u1} = -(U^*/\kappa) [1/(z - d_m) + \partial \Psi_m(\zeta_i) / \partial a_{u1}], \quad (11a)$$

$$\partial U_i / \partial a_{u2} = \ln(z - d_m) - \Psi_m(\zeta_i) + \Psi_m(\zeta_0) - \ln z_{0m}, \quad (11b)$$

$$\partial U_i / \partial a_{u3} = -(U^*/\kappa) [1/z_{0m} + \partial \Psi_m(\zeta_0) / \partial a_{u3}], \quad (11c)$$

$$\partial U_i / \partial a_{u4} = (U^*/\kappa) [\partial \Psi_m(\zeta_i) / \partial a_{u4} + \partial \Psi_m(\zeta_0) / \partial a_{u4}], \quad (11d)$$



Temperature and Humidity:

$$\partial T_f / \partial a_{t1} = 1, \quad (12a)$$

$$\partial T_f / \partial a_{t2} = \ln(z_i - d_h) - \Psi_h(\zeta_i) + \Psi_h(\zeta_0) - \ln z_{0h}, \quad (12b)$$

$$\partial T_f / \partial a_{t3} = -(T^*/\kappa) [1/z_{0h} + \partial \Psi_h(\zeta_0) / \partial a_{t3}], \quad (12c)$$

$$\partial T_f / \partial a_{t4} = -(T^*/\kappa) [1/(z_i - d_h) + \partial \Psi_h(\zeta_0) / \partial a_{t4}], \quad (12d)$$

$$\partial T_f / \partial a_{t5} = (T^*/\kappa) [1 - \partial \Psi_m(\zeta_i) / \partial a_{u5} + \partial \Psi_m(\zeta_0) / \partial a_{u5}], \quad (12e)$$

where  $a_{u1} = d_m$ ,  $a_{u2} = U^*/\kappa$ ,  $a_{u3} = z_{0m}$ ,  $a_{u4} = L$ ;  $a_{t1} = T_s$ ,  $a_{t2} = T^*/\kappa$ ,  
 $a_{t3} = z_{0h}$ ,  $a_{t4} = d_h$ ,  $a_{t5} = L$ .

For unstable conditions,

$$\partial \Psi_m(\zeta_i) / \partial a_{u1} = -(4/L) [\phi_m^2 / (\phi_m + 1)(\phi_m^2 + 1)],$$

$$\partial \Psi_m(\zeta_0) / \partial a_{u3} = 16/L [\phi_{0m}(\phi_{0m} + 1)(\phi_{0m}^2 + 1)],$$

$$\partial \Psi_m(\zeta_i) / \partial a_{u4} = (16/L^2) [ 1 / \phi_m(\phi_m + 1)(\phi_m^2 + 1) ],$$

$$\partial \Psi_m(\zeta_i) / \partial a_{u4} = -(16/L^2) [ 1 / \phi_{0m}(\phi_{0m} + 1)(\phi_{0m}^2 + 1) ],$$

$$\partial \Psi_h(\zeta_0) / \partial a_{t3} = 16/L [\phi_{0h}(\phi_{0h} + 1)],$$

$$\partial \Psi_h(\zeta_0) / \partial a_{t4} = 16/L [\phi_h(\phi_h + 1)],$$

$$\partial \Psi_m(\zeta_i) / \partial a_{u5} = 16/L^2 [(z_i - d_h) / \phi_h(\phi_h + 1)],$$

$$\partial \Psi_m(\zeta_i) / \partial a_{u5} = -16/L^2 [Z_{0+} / \phi_{0h}(\phi_{0h} + 1)].$$

For stable conditions, the derivatives of  $\Psi_{m,h,q}$ , with respect to  $d$  and  $Z_0$ , are all equal to  $5/L$ , and  $\partial \Psi_m(\zeta_i) / \partial L = 5(\zeta_i - \zeta_{0i}) / L^2$ .

Similarity is assumed between heat and moisture transfer; **therefore**, for moisture, in (12) expressions in  $T$  can be replaced by expressions in  $Q$ . This provides the set of equations for the fits to the moisture data.

Figure 1 is a flow chart of the procedure for fitting the data to the Monin-Obukhov equations. The initialization of parameters includes specifying certain physical constants (e.g.,  $g = 9.81 \text{ m/s}^2$ ), and setting counters and merit functions to starting values. Initial guesses for  $a_u$ ,  $a_t$ ,  $a_q$  are required to start the calculations. It is sufficient to use climatological data (e.g.,  $d$  and  $Z_0$ ) for initial values; or, if the height ( $h_{vw}$ ) of the vegetation is known, any of the empirical relationships relating  $h_{vw}$  to  $d$  and  $z_0$  (Brutsaert, 1982)

can be used. Actually, the Levenberg-Marquardt method is somewhat insensitive to whatever starting values are used, although at times, some experimentation may be necessary. Another way to start the procedure is to first use a reduced set of parameters (assuming all  $d$ 's and  $z_0$ 's are equal), and use the results from this run as starting values to calculate the full set of parameters in (11) and (12). Assuming equivalence of all  $d$ 's and  $z_0$ 's is the standard approach of profile analysis, and the Levenberg-Marquardt based procedure (hereafter abbreviated LMP) can be viewed as an extension of this technique.

#### 4. Experiments on Synthetic Data

To test this procedure, we used a synthetic data set that was developed by arbitrarily choosing parameters for  $U^*$ ,  $T^*$ ,  $Q^*$ ,  $L$ , and so forth (Table Ia). In this experiment, we only used wind and temperature data. Next, we selected a logarithmic (base 2) height range of 1 to 32 m for the calculations. Finally, we calculated profiles of  $U$ ,  $T$ ,  $Q$  from the values in Table Ia and (1) through (3). This was all done by using a commercial spreadsheet application (Quattro Pro, version 6.01) on a stand-alone, desktop PC (486 model). We call the profiles calculated in this way synthetic profiles of  $U$ ,  $T$ , and  $Q$ . The results are given in Table Ia for three different cases corresponding to different values of  $z_{0h}$  ( $= 0.09, 0.009, 0.0009$  m) and a single value of  $z_{0m}$  ( $= 0.09$  m).

Using a separate method, we coded the Levenberg-Marquardt procedure described in the last section - and diagrammed in Figure 1- in FORTRAN and compiled the program on a Sun Workstation (OS 5.0). We then ran the program to fit the profiles of Table Ia. Starting with an initial guess of the values given in Table Ia (usually one-half to a full order of magnitude larger or smaller than the actual values), the program was run until convergence or until the number of iterations exceeded 100. In all the calculations done for this paper, the number of iterations usually was less than 10, seldom exceeded 20, and never reached 50. Each iteration consisted of a set of calculations of  $U, T, Q$ , and all the associated  $a$  values in Table Ia. At the end of each iteration, the results were tested for convergence to see if another iteration was required. If the iteration test failed, the  $a$  values were changed and the profile computations redone. To test convergence, we first calculated the Monin-Obukhov scale height ( $L_f$ ) from the LMP. We call  $L_f$  the fitted value of  $L$ . Next, we calculated  $L$  from the separate calculated values of virtual temperature,  $T_v$ , specific humidity,  $q^*$ ,  $T^*$ , and  $T_{avg}$ , since  $L$  is:

$$L = U_*^2 T_v / \kappa g (T^* + 0.61 T_{avg} q^*). \quad (13)$$

This value of  $L$  we call the calculated value of  $L_c$ . We stress here that these two values of  $L$  are calculated separately: one as a result of the LMP fitting process ( $L_f$ ) and the other from direct calculation ( $L_c$ ) of fitted values. In theory, these two values should be equal. Therefore, we accept convergence of the solutions

when  $\varepsilon = \text{abs}(L_f - L_c) < 10^{-5}$ . We note that other convergence tests are possible; for example, convergence is obtained when some calculated parameter (e.g.  $T^*$ ) changes by less than some predetermined amount (e.g.  $10^{-5}$ ) from one iteration to the next. In tests, we have found no significant difference between this approach and the one we have used here. We prefer to use the  $L_f, L_c$  test because of the consistency of the notion that the two values should be nearly equal.

For each iteration, the profiles of U, T, and Q were calculated. Originally, the first LMP calculations used synthetic wind and temperature profiles calculated to 5 decimal places. When the 5 decimal place numbers were used as input in the Levenberg-Marquardt procedure, the standard deviations between the LMP calculated profiles and the synthetic data were extremely small, the smallest standard deviations being on the order of ( $10^{-5}$  to  $10^{-7}$ ). In other words, when the data is nearly perfect, the LMP fits the data nearly perfectly. This includes calculated values of  $U^*, T^*, Q^*, T_s, Q_s, d_m, d_h, d, \bar{m}, z_{0h}, z_{0q},$  and L. We show these results in Tables Ia, b,c,d. We also truncated the 5 decimal values of U, T, and Q to 2 decimal places (Table Ic) and used these values as input to the LMP. This approach serves as a rough indicator of the effects of measurement error on the effectiveness of the LMP (Table Id). The synthetic and calculated wind and temperature profiles in all the tables agree exactly in almost every case, and the surface layer values agree within a fraction of a percent.

These results indicate that the Levenberg-Marquardt procedure is fairly robust, and - in principle - capable of discriminating among different values of  $d_m$ ,  $d_h$ ,  $d_q$  and  $z_{0m}$ ,  $z_{0h}$ , and  $z_{0q}$ . As we shall see, differences in  $d$  and  $Z$ . affect the estimation of convective (sensible and latent) heat flux densities whenever they are calculated from resistance or drag coefficient type expressions.

## 5. Application to Actual Data

The LMP works well on synthetic (or made-up) data sets. In a sense, the process of obtaining solutions to these self-contained, made-up physical systems comprises a nearly closed method of analysis, because the answers are known to a given precision, and any imperfections in results are attributable mostly to the inexactness of the LMP procedure itself. Also, the assumption is made that the similarity equations are perfectly appropriate for the analysis. Testing the procedure on actual data sets is another matter. Errors occur in measurement, and there is always some lack of certainty in the appropriateness of the similarity equations to represent conditions at the field site. This has to do with sufficient fetch to the instrument, the inhomogeneity of the surface surrounding the site, and other matters. The real world is an open physical system and the answers are not as clear cut. However, we can compare our method with the results from other field

studies to see if our answers are nearly the same, and we do so in this section.

### 5.1 Petawawa Experimental Forest.

In 1968, measurements of wind speed and temperature were made in a Canadian forest over a mixed stand of mature red and white pine with a surface density of about 620 trees per ha. The measurements were obtained on a tower at 5 heights: 26, 31, 37, 46, and 61 m. The height of the trees averaged 21 m. Lo (1977), Kramm (1989), and Haenel (1993) analyzed the data with their own methods of computing wind and temperature profiles and surface layer parameters. Haenel (1993) summarized the results in Table II of his paper. The goodness of the fits between the measurements and calculated profiles was determined by computing a measure of scatter, or standard deviation (Panofsky and Brier, 1968):

$$s_{\chi} = \sqrt{(1/n) \sum_{i=1,n} (\chi_{im} - \chi_{ic})^2} , \quad (14)$$

where  $\chi_{im,c}$  refers to either a measurement (m) or calculated (c) value of a profile parameter ( $\chi = U$  or  $T$ ) at the height  $z_i$ , and  $n$  is the total number of measurements. Haenel's (1993) method was found to yield the best fits between the measured and calculated profile values.

Using the same data base, we applied the LMP to the 4 sets of profile data shown in Lo (1977), Kramm (1989), and Haenel (1993). For this case, we used the same assumptions these previous investigators did, i.e.,  $d = d_m = d_h$  and  $Z_u = z_{0m} = z_{0h}$ . This restriction allowed us to fit the data with less than the full set of 4 or 5 parameters each for U and T. Instead, we used 3 parameters ( $U_s, d, \text{ and } Z_u$ ) for the U profile fit, and 2 parameters ( $T_s, T_g$ ) for the T profile fit. Our results are compared with Haenel's (1992) in Table II. Our results are equal to or slightly better than Haenel's in all cases. We also tried using Hogstrom's (1988) modification of Dyer's (1974) formulae and Brutsaert's (1992) formulae for  $\Psi_m$  and  $\Psi_h$  to fit the data. There was no significant improvement in using Hogstrom's (1988) modified formulae over Dyer's (1974), and Brutsaert's (1992) formulae resulted in fits slightly worse than Haenel's (1993).

If this was all we could expect from the LMP, then we would have another profile analysis technique that produced answers rapidly and accurately. By relaxing the restriction that all d's and  $Z_u$ 's are equal and using the full set of equations in (11) and (12), we calculate individual values of d and Z. for U, T, and Q in the sections below. Note that this can be done with profile data only, and not with the assistance of ancillary data sets like surface temperature measurements from infrared radiometers.



## 5.2 University of California at Davis Field

We tested the full set of (11) and (12) on a data set gathered by the University of California at Davis (UC Davis) staff at the Hydrometeorological Field Site at Davis and reported by Morgan *et al.* (1971). This consisted of a set of measurements of wind speed, temperature, and absolute humidity at up to 7 levels over a flat field covered by short grasses, Morgan *et al.* (1971) list data for the summers of 1966 and 1967, They calculated a zero plane displacement height ( $d$ ) of about 10 cm during June 1966 and 15 cm during September 1967. The aerodynamic roughness length ( $z_0$ ) was calculated as **0.94** cm in June 1966 and 0.88 cm in September 1967. We reanalyzed 10 profile data sets during June 1966 and September 1967 using the LMP. The results are given in Tables IIIa and IIIb. The profiles from the UC Davis report are listed in the Appendix. Note that the standard deviations between the measured and LMP calculated profiles are quite good, and are about an order of magnitude better than the results shown in Table II for the forested region of Lo's (1977) data sets.

For the June 2, 1966 afternoon data, we see that the separate values of  $d_m$ ,  $d_h$ , and  $d_q$  average about 10, 13, and 12 cm respectively as opposed to the single value of 10 cm quoted above. Likewise for the  $z_0$ , we find that  $z_{0m}$ ,  $z_{0h}$ , and  $z_{0q}$  average about

0.90, 0.04, and 0.40 cm respectively, versus a previously calculated single value of 0.94 cm. For the September 28, 1967 morning data, we find that the  $d_m$ ,  $d_h$ ,  $d_q$  values average about 15, 13, and 20 cm. The  $z_{0m}$ ,  $z_{0h}$ ,  $z_{0q}$  values average about 0.61, 0.04, and 0.45 cm. The  $d$  and  $Z$ . results are fairly consistent between these two data sets that reflect different annual and diurnal periods. Also, except for  $d_q$  in the morning data, the  $d$  values all agree within 10-20% or so of each other for each data set. The  $Z$ . values are more variable, particularly  $z_{0h}$ . The ratio of the three  $z_0$  values indicate a range of from 7 to 2000 for  $z_{0m}/z_{0h}$ ; from 1/2 to 6 for  $z_{0m}/z_{0q}$ ; and from 4 to 600 for  $z_{0q}/z_{0h}$ .

Although values for  $z_{0q}/z_{0h}$  and  $z_{0m}/z_{0q}$  are difficult to find in the literature, a number of studies exist for  $z_{0m}/z_{0h}$ . Kustas et al (1989) found a value of 270 over a sparse canopy in Owens Valley California. Betts and Beljaars (1993) found  $z_{0m}/z_{0h}$  to be about 16 from an analysis of aircraft and surface data from the 1978 FIFE experiment in Kansas. They estimated an error range of 7-35. Hignett (1994) at the U.K. Meteorological Office field site in Cardington, Bedfordshire, England and Duynkerke (1992) at the Cabauw site in the Netherlands found some exceptionally high ( $\sim 105$ ) values of  $z_{0m}/z_{0h}$  in their analyses. These studies and the further results of our findings for  $z_{0m}/z_{0q}$  and  $z_{0q}/z_{0h}$  indicate that assuming equality for all  $d$ 's and  $Z$ 's is not warranted. In the next section, we show how calculations of convective heat flux densities are affected when  $d$  and  $Z$ . values differ.

We also analyzed a number of nighttime (stable conditions) profiles for June 21 1966. We found that these profiles yielded about the same values for  $d$  and  $Z$ . that were obtained in Tables IIIa and IIIb. There were some difficulties in analyzing the data under stable conditions when winds were light (i.e. much less than 1 m/s) and also, many times the profiles of temperature and humidity were dissimilar. Under the latter conditions, temperature values increased with height from the surface while humidity values decreased with height. These conditions produced humidity values (mostly negative values of  $d$ ) that were inconsistent with the values found in the unstable analysis. Since convective heat flux densities for stable conditions are small anyway, separate evaluation of  $d$  and  $Z$ . for momentum, heat, and moisture is probably not important under these conditions. As shown in the next section, assuming  $d$  and  $Z$ . are the same for momentum, heat, and moisture transfer - when flux densities are usually large - can significantly affect heat flux calculations,

## 6. Computing Convective Heat Flux Densities

Convective heat flux densities in the surface layer are sometimes calculated by modelers by using either the resistance or bulk transfer methods (Garrat, 1992). Here, we show how heat flux density calculations are affected by the choice of roughness lengths, and - mainly for notational convenience - we use the bulk transfer method to make the point, The bulk transfer expressions for momentum, heat, and humidity flux densities are:

$$\tau = \rho C_d U_r^2, \quad (15)$$

$$H = \rho c_p C_h U_r (T_s - T_r), \quad (16)$$

$$LE = L_s C_q U_r (Q_s - Q_r) \quad (17)$$

where  $r$  refers to the reference height at  $z_r$ ,  $\tau$  is the surface shear stress, and the other symbols are defined as before. The bulk transfer coefficients are:

$$C_d = \kappa^2 / [\ln((z_r - d_m)/z_{0m}) - \gamma_m(g)] \quad (18)$$

$$C_h = \kappa^2 / [\ln((z_r - d_m)/z_{0m}) - \Psi_m(\xi)] [\ln((z_r - d_h)/z_{0h}) - \Psi_h(\xi)] \quad (19)$$

$$C_q = \kappa^2 / [\ln((z_r - d_m)/z_{0m}) - \Psi_m(\xi)] [\ln((z_r - d_q)/z_{0q}) - \Psi_q(\xi)] \quad (20).$$

We computed  $H$ ,  $LE$ ,  $C_d$ ,  $C_h$ ,  $C_q$  from (15) through (20) for all the periods of the UC Davis data analyzed in the previous section. The results are shown in Figures 2a and 2b. Both figures indicate the influence of the disparate values of  $z_{0m}$ ,  $z_{0h}$ ,  $z_{0q}$ . If we assume that  $d_m = d_h = d_q$  and  $z_{0m} = z_{0h} = z_{0q}$  then  $C_d = C_h = C_q$ , a plot of the ratio of all the bulk transfer coefficients would be a constant value of 1 (i.e.,  $C_d/C_h = C_d/C_q = C_h/C_q = 1$ ). This is not what Figure 2 shows. When we take into account the differences among  $d$  and  $Z$ . for momentum, heat, and moisture transfer, Figure 2 shows that  $C_d/C_h$  is about 2,  $C_d/C_q$  is somewhat more than 1, and  $C_h/C_q$  is about 1/2. Moreover, from (16) and (17), the Bowen ratio ( $\beta = H/LE$ ) is directly proportional to  $C_h/C_q$ . This means that for the UC Davis site – by assuming that all  $d$  and  $Z$ . values are equal –  $\beta$  could be overestimated by about 100% and that  $H$  (or  $LE$ ) could

be consistently overestimated (or underestimated) by significant amounts.

## 7. Summary and Conclusions

The principal result of this study is that:

- . Analysis of the UC Davis data shows that the usual practice of equating all the  $d$  and  $z_0$  values for momentum, heat, and humidity can be the source of significant errors in calculating  $H$  and  $LE$  from the bulk transfer method. The same conclusion can be drawn for the resistance method since the mathematical formalism of deriving the two methods involves using similar kinds of expressions. It is important to be able to discriminate the differences among the different values of  $d$  and  $z_0$  if one intends to model the surface flux density behavior in the atmospheric boundary layer.

Additionally, we have shown that:

- . The non-linear Levenberg-Marquardt procedure of fitting profile parameters to field data is a robust and accurate means of calculating roughness lengths, displacement heights, and convective heat flux densities;
- . Separate values of  $d$  and  $z_0$  can be calculated from profile data without recourse to ancillary measurements, e.g. brightness temperature measurements - made by use of an infrared

QA  
sub:

radiometer (IRR) - to extend the profile data. The average surface temperatures derived from IRR measurements may not represent the same temporal or spatial variations of the wind, temperature, and humidity measurements made on the profile instrument mount. Profile sensors may sample source regions for their signals at distances hundreds of meters or kilometers upwind of their location (Schmid and Oke, 1990),

Measurements are usually averaged over 20 minutes to one hour periods. IRR measurements are not always so carefully made, and may represent an area a few hundred square meters around the profile sensors with a sampling period of 5 or 10 minutes. There is always the problem of what surface the surface temperature represents particularly if the surface of interest is anything other than uniform, bare ground under clear skies. IRR measurements are also sensitive to variations in emissivity (Feijt and Kohsiek, 1995) and viewing angle .

Furthermore, since IRR's are relatively costly, it may be a better investment to purchase additional anemometers, and temperature and humidity sensors to add additional levels to the profile system. Wieringa ( 1993) estimates at least 4 levels of instrumentation are necessary to determine  $z_0$  within a factor of 2. For these reason, separate calculation of  $d$  and  $z_0$  values is probably best done from profile data alone.

### Figure Captions

Figure 1. Flowchart depicting Levenberg-Marquardt Procedure (LMP).

Figure 2a. Ratio of bulk transfer coefficients for June 2, 1966 field site at UC Davis.

Figure 2b. Ratio of bulk transfer coefficients for September 28, 1967 field site at UC Davis.

### Table Captions

Table 1a. Synthetic data base for winds and temperatures with three different cases ( $z_{0h} = 0.09, 0.009, 0.0009$  m). Data for 5 decimal places.

Table 1b. Wind, temperature, and surface layer parameters fitted to data in Table 1 a by Levenberg-Marquardt procedure.

Table 1c. Synthetic data base for winds and temperatures with three different cases ( $z_{0h} = 0.09, 0.009, 0.0009$  m). Data of Table 1 a rounded to two decimal places.

Table Id. Wind, temperature, and surface layer parameters fitted to data in Table 1 c by Levenberg-Marquardt procedure.

Table II. Comparison of Haenel's method versus Levenberg-Marquardt procedure (LMP). In the LMP, we used 3 parameters to fit winds ( $z_o$ ,  $d$ ,  $U_*$ ) and 2 parameters for temperature ( $T_*$ ,  $T_g$ ).

Table III. LMP results for the afternoon of June 9, 1966 at UC Davis field.

Table IIIb. LMP results for the morning of September 28, 1967 at UC Davis field.

Table AI. Wind, temperature, and absolute humidity values for June 2, 1966 at UC Davis. Seven levels of wind and temperature data and six levels of humidity data for each time. Heights are in meters.

Table AII. Wind, temperature, and absolute humidity values for September 28, 1967 at UC Davis.



## References

Beal, E. M. K., 1967: Numerical methods in *Nonlinear* Programming (J. Abadie editor). North Holland Publishing Co., Amsterdam, pp 135-205.

Betts, A.K. and A.C.M. Beljaars, 1993: Estimation of effective roughness length for heat and momentum from FIFE data. *Atmos. Research*, 30,251-261.

Brutsaert, W. A., 1982: *Evaporation into the Atmosphere*. Reidel, Dordrecht, 299 pp.

Brutsaert, W. A., 1992: Stability correction functions for the mean wind speed and temperature in the unstable surface layer. *Geophys. Res. Letters*, **19,469-472**.

Duynkerke, P. G., 1992: The roughness length for heat and other vegetation parameters for a surface of short grass. *J. Appl. Meteor.*, 31, 579-586.

Dyer, A. J., 1974: A review of flux-profile relationships. *Boundary-Layer Meteorol.*, 7,363-372.

Feijt, A.J. and W. Kohsiek, 1995: The effect of emissivity variation on surface temperature determined by infrared radiometry. *Boundary-Layer Meteorol.*, 72,323-327.

Garratt, J. R., 1992: *The atmospheric boundary layer*. Cambridge University Press, Cambridge, 316 pp.

Haenel, H.-D., 1993: Surface-layer profile evaluation using a generalization of Robinson's method for the determination of  $d$  and  $z_0$ . *Boundary-Layer Meteorol.*, 65,55-67.

Hignett, P., 1994: Roughness lengths for temperature and momentum over heterogeneous terrain. *Boundary-Layer Meteorol.*, 68,225-236.

Hogstrotn, U., 1988: Non-dimensional wind and temperature profiles in the atmospheric surface layer: are-evaluation. *Boundary-Layer Meteorol.*, 42, 55-78.

Kramm, G., 1989: The estimation of the surface-layer parameters from wind velocity, temperature, and humidity profiles by least-squares methods. *Boundary -Layer Meteorol.*, 48,315-327.

Kuester, J.L. and J.H. Mize, 1973: *Optimization techniques with Fortran*. McGraw-Hill Book Co., New York, pp. 240-250.

Kustas, W. P., B.J. Choudhury, M.S. Moran, R.J. Reginato, R.D. Jackson, L.W. Gay, and H.J. Weaver, 1989: Determination of sensible heat flux over

sparse canopy using thermal infrared data. *Agric. Forest Meteorol.*, 44, 197-216.

Lo, A. K., 1977: An analytical-empirical method for determining the roughness length and zero-plane displacement. *Boundary -Layer Meteorol.*, 12, 141-151.

Morgan, D. L., W.O. Pruitt, and F.J. Lourence, 1971: Analyses of energy, momentum, and mass transfers above vegetative surfaces. ECOM 68-G 10-F. Report prepared by Department of Water Science and Engineering, University of California at Davis, for United States Army Electronics Command, Atmospheric Sciences Laboratory, Fort Huachuca, Arizona.

Panofsky, H.A. and G.W. Brier, 1968: *Some applications of statistics to Meteorology*. Penn State University.

Press, W. H., B.P. Flannery, S.A. Teukolsky, W.T. Vetterling, 1986: *Numerical Recipes: The art of scientific computing*. Cambridge University Press, Cambridge, pp. 521-528.

Robinson, S. M., 1962: Computing wind profile parameters. *J. Atm. Sci.*, 19, 189-190.

Schmid, H.P. and T.R. Oke, 1990: A model to estimate the source area contributing to turbulent exchange in the surface layer over patchy terrain. *Quart. J. Roy. Meteorol. Soc.*, 116, 965-988.

Wieringa, J., 1993: Representative roughness parameters for homogeneous terrain. *Boundary -Layer Meteorol.*, 63,323-363.

*Acknowledgment.* The research described in this paper was carried out at the Jet Propulsion Laboratory, California Institute of Technology, under a contract with the National Aeronautics and Space Administration. Reference herein to any specific commercial product, process or service by trade name, trademark, manufacturer, or otherwise, does not constitute or imply its endorsement by the United States Government or the Jet Propulsion Laboratory, California Institute of Technology,

	Case 1		Case 2		Case 3	
Height (m)	U (m/s)	T (C)	U (m/s)	T (C)	U (m/s)	T (C)
1	1.19806	19.6793	1.19713	16.9571	1.19617	14.162
2	1.56995	19.119	1.56844	16.3986	1.56687	13.6053
4	1.866	18.7335	1.86392	16.0146	1.86176	13.2229
8	2.10915	18.4633	2.10656	15.7455	2.10387	12.9549
16	2.31142	18.2727	2.30838	15.5558	2.30523	12.7661
32	2.48064	18.1381	2.47721	15.4218	2.47366	12.6327
Surface layer parameters						
z0m (m)	0.09		0.09		0.09	
z0h (m)	0.09		0.009		0.0009	
L (m)	-9.07		-8.99		-8.9	
U* (m/s)	0.25		0.25		0.25	
T* (c)	-0.5		-0.5		-0.5	
Ts (C)	21.84		21.84		21.84	
dm (m)	0.2		0.2		0.2	
dh (m)	0.2		0.2		0.2	

Table IA

	Case 1		Case 2		Case 3	
Height (m)	U (m/s)	T (C)	U (m/s)	T (C)	U (m/s)	T (C)
1	1.19805	19.6793	1.19713	16.9571	1.19617	14.162
2	1.56995	19.119	1.56844	16.3986	1.56687	13.6053
4	1.866	18.7335	1.86392	16.0146	1.86176	13.2229
8	2.10915	18.4633	2.10656	15.7455	2.10387	12.9549
16	2.31142	18.2727	2.30838	15.5558	2.30523	12.7661
32	2.48064	18.1381	2.47721	15.4218	2.47366	12.6327
Surface layer parameters						
z0m (m)	0.09		0.09	--	0.09	
z0h (m)	0.09		0.009		0.0009	
L (m)	-9.0717		-8.98713		-8.9004	
u' (m/s)	0.2439		0.2439		0.2439	
T* (c)	-0.48779		-0.4878		-0.4878	
Ts (C)	21.84		21.84		21.84	
dm (m)	0.2		0.2		0.2	
dh	0.2		0.2		0.2	

Table IB

J. Schieldge

	Case 1		Case 2		Case 3	
Height (m)	U (m/s)	T (C)	U (m/s)	T (C)	U (m/s)	T (C)
1	1.2	19.68	1.2	16.96	1.2	14.16
2	1.57	19.12	1.57	16.4	1.57	13.61
4	1.87	18.73	1.86	16.01	1.86	13.22
8	2.11	18.46	2.11	15.8	2.1	12.95
16	2.31	18.27	2.31	15.56	2.31	12.77
32	2.48	18.14	2.48	15.42	2.47	12.63
<b>Surface layer parameters</b>						
z0m (m)	0.09		0.09		0.09	
z0h (m)	0.09		0.009		0.0009	
L (m)	-9.07		-8.99		-8.9	
U* (m/s)	0.25		0.25		0.25	
T* (C)	-0.5		-0.5		-0.5	
Ts (C)	21.84		21.84		21.84	
dm (m)	0.2		0.2		0.2	
dh	0.2		0.2		0.2	

Table IC

	Case1		Case 2		Case 3	
Height (m)	U (m/s)	T (C)	U (m/s)	T (C)	U (m/s)	T (C)
1	1.2	19.69	1.2	16.93	1.2	14.16
2	1.57	19.12	1.57	16.39	1.57	13.61
4	1.87	18.73	1.86	16.01	1.86	13.22
8	2.11	18.46	2.11	15.75	2.1	12.95
16	2.31	18.27	2.31	15.56	2.3	12.76
32	2.48	18.14	2.48	15.42	2.47	12.63
<b>Surface layer parameters</b>						
z0m (m)	0.08846		0.09186		0.09014	
z0h (m)	0.08935		0.00851		0.00095	
L (m)	-9.01097		-9.16974		-8.84322	
U* (m/s)	0.24306		0.24446		0.2441	
T* (c)	-0.48768		-0.48107		-0.49174	
Ts (C)	21.84		21.84		21.84	
dm (m)	0.20621		0.1843		0.19205	
dh (m)	0.20621		0.1843		0.19205	

Table ID

J. Schieldge

	Haenel's Results					
	z0 (m)	d (m)	U* (m/s)	T* (K)	Su (m/s)	St (K)
Data Set 1	2.606	10.8	0.648	-1.0276	0.023	0.028
Data Set 2	3.712	10,389	1.073	-0.1848	0.028	0.024
Data Set 3	2,498	11.217	0.988	-0.6161	0,036	0.051
Data Set 4	1.509	14.61	0.928	-0.3814	0.02	0.057
	Our Results (L)					
Data Set 1	2.571	10,903	0.641	-0.9487	0.022	0.024
Data Set 2	3.712	10.39	1,073	-0.1848	0.028	0.024
Data Set 3	2.483	11.277	0.987	-0.6161	0.036	0.051
Data Set 4	1.506	14.628	0.928	-0.3817	0.02	0.057

Table II

J. Schieldge

Time (LT)	1400	1430	1500	1 5 3 0	1600
L	-8.6671	-59.1915	-159.882	-230.618	-493.37
dm	0.069453	0.10611	0.10565	0.11026	0.10449
dh	0.08758	0.17353	0.15821	0.12322	0.13134
dq	0.15879	0.14229	0.09651	0.10297	0.10189
z0m	0.01164	0.00768	0.00846	0.0085	0.0085
z0h	0.001735	0.000081	0.000017	0.000009	0.000003
Zoq	0.00738	0.0051	0.00414	0.00217	0.00141
Su	0.00413	0.00663	0.00659	0.00813	0.00789
St	0.00356	0.00732	0.00903	0.00256	0.00438
Sq	0.00517	0.00014	0.00036	0.00023	0.00005

Table III A

Time (LT)	1000	1030	1100	1 1 3 0	1200
L	-86.8328	-13,3161	-38.2658	-31.227	-31.8582
dm	0.17168	0.15469	0.15068	0.15592	0.13987
dh	0.14978	0.1137	0.1342	0.15445	0.10558
dq	0.23596	0.144	0.18994	0.23564	0.18529
z0m	0.00623	0.00559	0.00637	0.00529	0.00709
z0h	0.000003	0.00028	0.001316	0.000045	0.000166,
Zoq	0.0018	0.00889	0.00578	0.0024	0.00371
Su	0.00101	0.0025	0.00575	0.00504	0.00636
St	0.00361	0.00224	0.00322	0.00105	0.00198
Sq	0.00197	0.00213	0.00228	0.00273	0.00054

Table III B

J. Schieldge



## Appendix for UC Davis profile data

Time (LT)	1400	1430	1500	1530	1600
<b>Winds</b>	(m/s)				
0.25	1.1	2.1	2.85	3.1	3
0.35	1.27	2.47	3.38	3.7	3.55
0.5	1.42	2.81	3.85	4.22	4.05
0.7	1.55	3.1	4.26	4.7	4.5
1	1.69	3.37	4.68	5.13	4.9
1.4	1.8	3.64	5.02	5.55	5.3
2	1.9	3.87	5.4	5.95	5.7
<b>Temperature</b>	(c)				
0.25	22.61	22.45	21.67	21.57	21.2
0.35	22.36	22.25	21.55	21.48	21.15
0.5	22.16	22.08	21.43	21.4	21.12
0.7	21.99	21.95	21.33	21.33	21.1
1	21.84	21.85	21.25	21.26	21.06
1.4	21.71	21.76	21.19	21.21	21.04
2	21.6	21.68	21.13	21.15	21.01
<b>Humidity</b>	(g/cubic cm) x 10A6				
0.35	8	8.5	8.48	8.37	8.56
0.5	7.38	7.99	8.08	8.05	8.3
0.7	6.87	7.57	7.75	7.8	8.07
1	6.46	7.2	7.43	7.55	7.85
1.4	6.1	6.86	7.14	7.31	7.64
2	5.91	6.54	6.82	7.07	7.44

Table AI

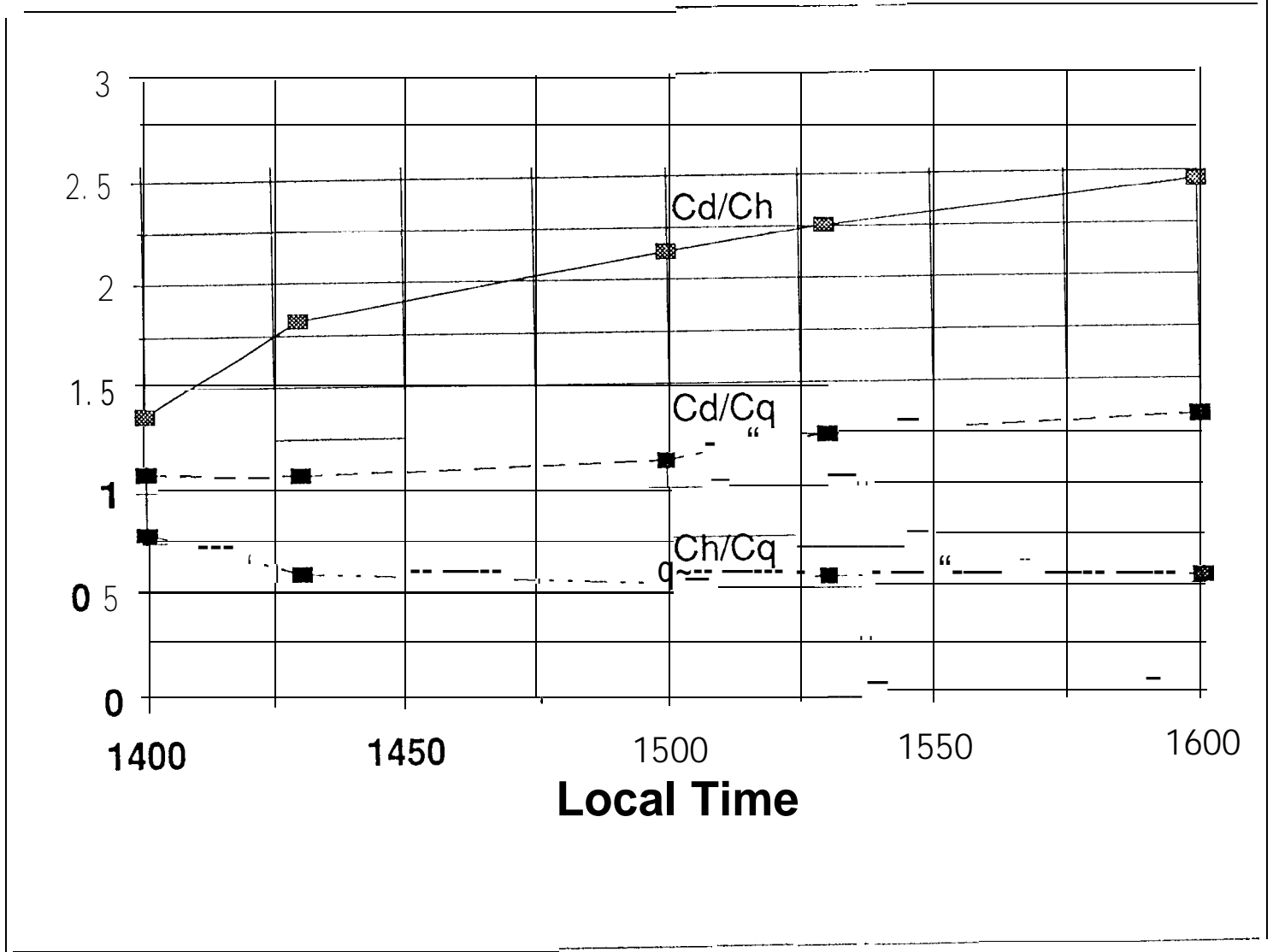
J. Schiedge

Time (LT)	1000	1030	1100	1130	1400
<b>Winds</b>	(m/s)				
0.25	1.58	1.08	1.24	1.04	1.14
0.35	2.07	1.34	1.55	1.3	1.4
0.5	2.46	1.55	1.8	1.5	1.63
0.7	2.76	1.71	1.99	1.65	1.8
1	3.04	1.85	2.19	1.81	1.95
1.4	3.26	1.97	2.33	1.94	2.11
2	3.48	2.09	2.5	2.05	2.25
<b>Temperature, (c)</b>					
0.25	23.57	24.75	26.12	27.09	27.62
0.35	23.48	24.58	26.02	27	27.53
0.5	23.41	24.44	25.94	26.93	27.46
0.7	23.34	24.33	25.87	26.88	27.4
1	23.29	24.23	25.82	26.83	27.34
1.4	23.24	24.14	25.76	26.79	27.29
2	23.2	24.07	25.71	26.75	27.24
<b>Humidity</b>	(g/cubic cm) x 10 <sup>6</sup>				
0.35	15.68	16.46	17	16.6	17.35
0.5	15.07	15.78	16.2	15.6	16.49
0.7	14.62	15.18	15.54	14.89	15.82
1	14.23	14.71	14.98	14.3	15.25
1.4	13.94	14.31	14.55	13.88	14.78

Table AII

J. Schiedge

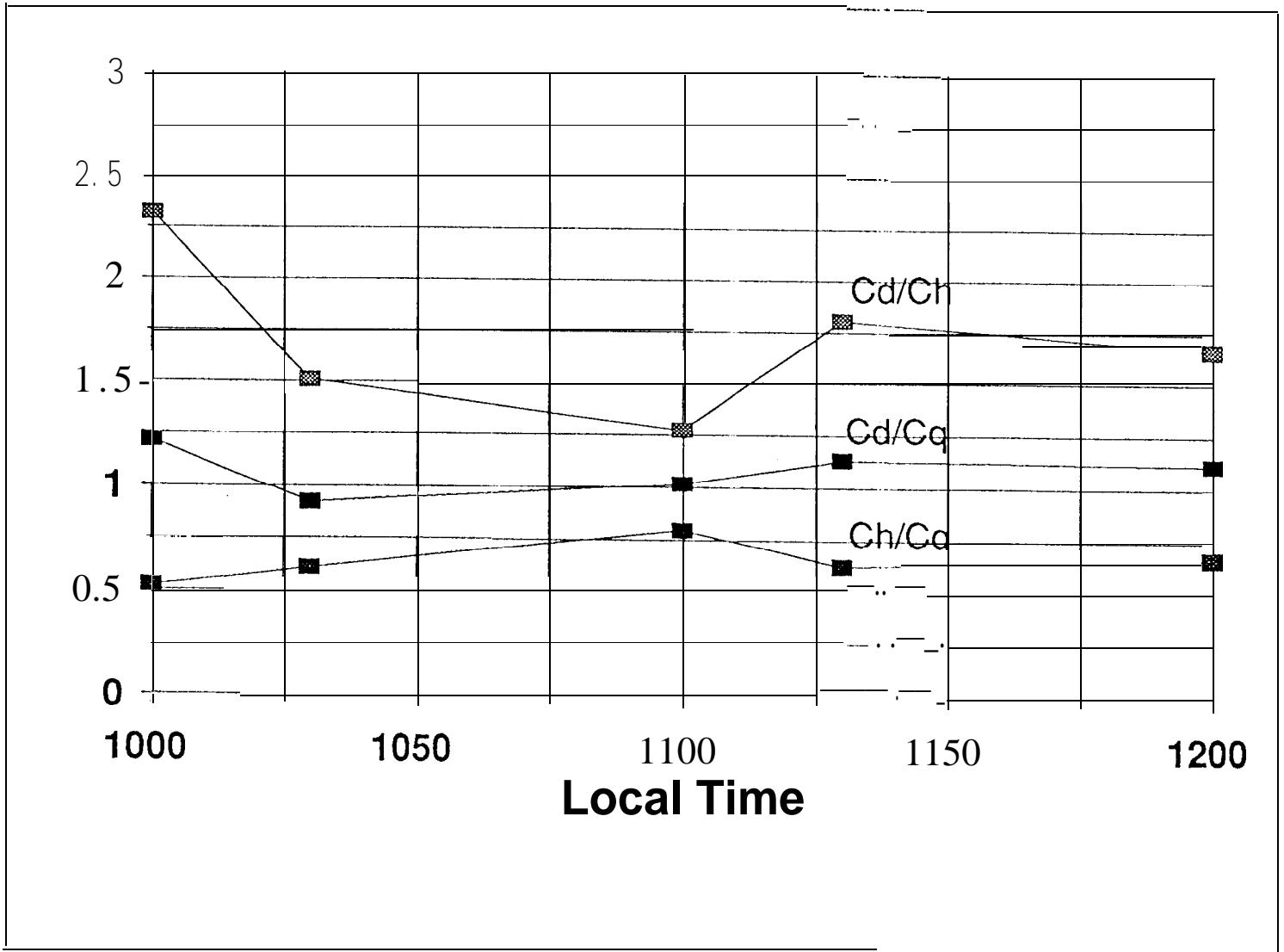
Orientation - top of figure



J. Schieldge

Figure 2a

Orientation - top of figure



J. Schieldge

Figure 2b